# Reaction and diffusion in dense nonideal plasmas

D. Kremp, M. Schlanges, M. Bonitz, and T. Bornath
*Universität Rostock, Fachbereich Physik, Universitätsplatz 3, O-2500 Rostock, Germany*

(Received 15 May 1992; accepted 3 August 1992)

The nonequilibrium properties of strongly coupled plasmas are investigated taking into account reaction and diffusion processes. The starting point is quantum kinetic equations for systems with chemical reactions involving many-body effects like screening, self-energy, and medium-dependent scattering. The influence of these effects on the kinetics of reaction and diffusion processes is discussed. Generalized expressions for the coefficients of impact ionization and diffusion are derived exhibiting a strong density dependence due to the many-body effects. Solving the reaction-diffusion equation (RDE) for a dense hydrogen plasma, nonlinear phenomena such as bistability, running ionization fronts, and droplet formation are obtained.

## I. INTRODUCTION

Dense nonideal plasmas are of interest from the theoretical point of view as well as from that of experimental investigations, e.g., in shock wave or laser compression.[1–4] In this paper, we consider the nonequilibrium properties of nonideal plasmas. We are especially interested in the influence of nonideality effects on the ionization kinetics and on diffusion.

Let us start our consideration with the following question: What is a nonideal plasma and which special effects may be expected in such a system? The behavior and the properties of a nonideal plasma are determined by the Coulomb interaction and the degeneracy. We have to account for degeneracy effects if the electron number density $n_e$ and the thermal wavelength $\Lambda_e$ fulfill the condition

$$n_e\Lambda_e^3 \geqslant 1, \quad \Lambda_e = \sqrt{2\pi\hbar^2/m_e k_B T}.$$

The Coulomb interaction is important in the "corner of correlation" which can be seen in Fig. 1. This area is enclosed by the parameter lines

$$n_e l^3 = 1, \quad r_s = 1.$$

Here $l = e^2/(k_B T)$ is the Landau length and $r_s = d/a_B$ is the Brueckner parameter with the mean particle distance $d$ and the Bohr radius $a_B$. In the corner of strong correlations many-particle effects may be expected, such as dynamical screening of the Coulomb interaction, dynamical self-energy, Pauli blocking, formation of bound states, and pressure ionization (Mott effect).[5,6]

All these effects influence the equilibrium and nonequilibrium properties of a plasma. Of special interest are reaction-diffusion processes, which means formation and decay of bound states in connection with diffusion. From the phenomenological point of view, such processes are described by coupled reaction-diffusion equations:

$$\frac{\partial n_a}{\partial t} + \nabla j_a = W_a(n_1,\ldots,n_f), \quad a = 1,2,\ldots,f, \tag{1}$$

with $j_a = -D_a \nabla n_a$ being the diffusion current and $W_a(n_1,\ldots,n_f)$ the source function describing the ionization kinetics. Reaction-diffusion equations are of general interest because they can serve as basic models for the description of evolution processes and structure formation in physics, chemistry, biology, and even for social sciences.[7–9] Therefore, the foundation of such reaction-diffusion equations from the fundamental equations of nonequilibrium statistical mechanics is an essential problem of the theory. Usually, the kinetic properties of many-particle systems are given by Boltzmann-like kinetic equations. But these equations can be applied to dilute systems only neglecting the nonideality effects mentioned above.

In order to describe the nonequilibrium properties of nonideal plasmas we have to start from generalized kinetic equations. As we will show, reaction-diffusion equations can be derived then with generalized expressions for the reaction rate and diffusion coefficients. Because of the nonideality, especially the diffusion coefficients $D_a$ as well as the source function of the chemical reactions $W_a$ become density dependent in a complicated nonlinear way. Therefore, nonlinear macroscopic phenomena like ionization fronts, phase separation, etc., can be expected.

The paper is organized as follows. In the first part (Sec. II), we present the generalized kinetic equations for chemically reacting systems which are applied then to nonideal plasmas. Using the hydrodynamic approximations, we derive reaction-diffusion equations and obtain microscopically founded expressions for the source function and the diffusion coefficient including nonideality effects in Sec. III. Finally, the influence of these many-body effects on the macroscopic behavior of dense plasmas is considered and nonlinear phenomena like nonlinear diffusion, bistability, running ionization fronts, and droplet growth are discussed (Secs. IV and V).

## II. KINETIC EQUATIONS FOR NONIDEAL MANY-PARTICLE SYSTEMS WITH CHEMICAL REACTIONS

Kinetic equations which take into account the formation and the decay of bound states are given in papers by Peletminski,[10] Lowry and Snider,[11] Klimontovich and Kremp,[12,13] McLennan,[14] and others. But these equations have to be generalized for the case of nonideal reactive systems where many-body effects must be taken into ac-

0899-8221/93/010216-14$06.00

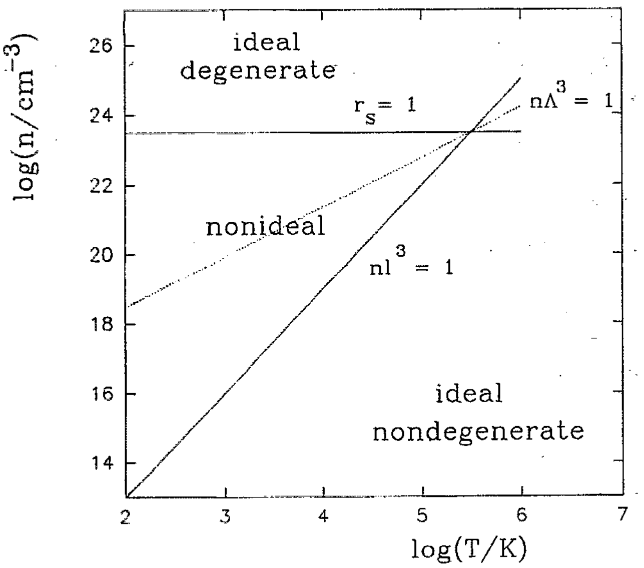

FIG. 1. Density–temperature plane showing three regions of qualitatively different behavior of plasmas. The area of strongly coupled plasma (so-called corner of correlations) is enclosed by the parameter lines $r_s = 1$ and $nl^3 = 1$.

count. This rather complicated problem was solved[15–17] using the method of nonequilibrium real-time Green's functions.

The result is the following kinetic equation for the Wigner distribution function $f_a$ of the free particles of species $a$

$$\left(\frac{\partial}{\partial t}+\frac{\partial E_a}{\partial p}\frac{\partial}{\partial r}-\frac{\partial E_a}{\partial r}\frac{\partial}{\partial p}\right)f_a(prt)$$

$$=\sum_b I_{ab}(p,r,t)+\sum_{bc} I_{abc}(p,r,t). \tag{2}$$

The single-particle energies on the left-hand side (lhs) are given by the dispersion relation

$$E_a(prt)=\frac{p^2}{2m_a}+\mathrm{Re}\,\Sigma_a^R(p\omega rt)\,|_{\hbar\omega=E_a(prt)}\,, \tag{3}$$

where $\Sigma_a^R(p\omega rt)$ is the retarded self-energy function. The latter gives the shift of the energy of an isolated particle due to the influence of the surrounding particles and therefore accounts for many-body effects in the kinetic equation. The energy shift can be calculated from a cluster expansion of the causal self-energy function. In a diagrammatic representation, it can be written in the form

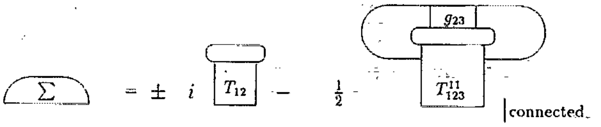

(4)

where the first term represents the two-particle ladder contribution and the second term accounts for the three-particle processes.

On the right-hand side (rhs) of the kinetic equation (2), the collisions between quasiparticles are taken into account. In the case that the free particles are Fermions, the quantum mechanical Boltzmann collision integral $I_{ab}$ is given by

$$I_{ab}(p_a,r,t)=\frac{1}{\hbar V}\int\frac{d^3p_b}{(2\pi\hbar)^3}\frac{d^3\bar{p}_a}{(2\pi\hbar)^3}\frac{d^3\bar{p}_b}{(2\pi\hbar)^3}\,|\langle p_ap_b|T_{ab}|\bar{p}_a\bar{p}_b\rangle|^2 2\pi\delta(E_{ab}-\bar{E}_{ab})[\bar{f}_a\bar{f}_b(1-f_a)(1-f_b)$$
$$-(1-\bar{f}_a)(1-\bar{f}_b)f_af_b]. \tag{5}$$

The three-particle collision integral can be written as

$$I_{abc}(p_a,r,t)=\frac{1}{2}\frac{1}{\hbar V}\sum_\kappa\int\frac{d^3p_b}{(2\pi\hbar)^3}\frac{d^3p_c}{(2\pi\hbar)^3}\,d(\kappa\bar{\alpha})\,|\langle p_ap_bp_c|T_{abc}^{0\kappa}|\kappa\bar{\alpha}\rangle|^2 2\pi\delta(E_0-\bar{E}_\kappa)(\bar{f}_\kappa N_0-\bar{N}_\kappa f_af_bf_c)$$
$$+\frac{1}{2\hbar V}\sum_{n_{bc}}\sum_\kappa\int\frac{d^3P_{bc}}{(2\pi\hbar)^3}\,d(k\bar{\alpha})\,|\langle p_aP_{bc}n_{bc}|T_{abc}^{1k}|\kappa\bar{\alpha}\rangle|^2 2\pi\delta(E_1-\bar{E}_\kappa)(\bar{f}_\kappa N_1-\bar{N}_\kappa f_aF_{n_{bc}}). \tag{6}$$

The integrals $I_{abc}$ contain all the possible three-body scattering processes with free and bound particles. Especially, breakup and formation reactions are taken into account. In order to classify the different collision processes, we have applied the notation of multichannel scattering theory which is explained in Table I.

All processes are included by the sum over the channel numbers $\kappa$ where $\int d(\kappa\alpha)$ stands for the integration over the dynamical variables of the corresponding channel state $|\kappa\alpha\rangle$. Here, $|p\rangle$ and $|jP\rangle$ are single-particle states and two-particle bound states, respectively, $f_a=f_a(p,r,t)$ and $F_j=F_j(P,r,t)$ denote the corresponding distribution functions normalized with respect to the number densities of free and bound particles, respectively.

The dynamics of the scattering processes enter the collision integrals via two- and three-particle $T$ matrices. The two-particle $T$ matrix is determined by the generalized Lippmann–Schwinger equation

$$T_{ab}(z)=V_{ab}+V_{ab}\,\frac{(1-f_a-f_b)}{z-H_{ab}^{\mathrm{eff}}}\,V_{ab}\,, \tag{7}$$

where $H_{ab}^{\mathrm{eff}}$ is an effective Hamiltonian

$$H_{ab}^{\mathrm{eff}}=E_a+E_b+(1-f_a-f_b)V_{ab}\,. \tag{8}$$

TABLE I. Reaction channels, asymptotic scattering states, channel energies, distribution functions, and phase space occupation factors for the three-body scattering processes contained in the integral $I_{abc}$.

| $\kappa$ | channel | $\vert\kappa\alpha\rangle$ | $E_\kappa$ | $f_\kappa$ | $N_\kappa$ |
|---|---|---|---|---|---|
| 0 | $a+b+c$ | $\vert p_a\rangle\vert p_b\rangle\vert p_c\rangle$ | $E_a+E_b+E_c$ | $f_af_bf_c$ | $(1-f_a)(1-f_b)(1-f_c)$ |
| 1 | $a+(b+c)$ | $\vert p_a\rangle\vert n_{bc}P_{bc}\rangle$ | $E_a+E_{nP_{bc}}$ | $f_aF_{n_{bc}}$ | $(1-f_a)(1+F_{n_{bc}})$ |
| 2 | $b+(a+c)$ | $\vert p_b\rangle\vert n_{ac}P_{ac}\rangle$ | $E_b+E_{nP_{ac}}$ | $f_bF_{n_{ac}}$ | $(1-f_b)(1+F_{n_{ac}})$ |
| 3 | $c+(a+b)$ | $\vert p_c\rangle\vert n_{ab}P_{ab}\rangle$ | $E_c+E_{nP_{ab}}$ | $f_cF_{n_{ab}}$ | $(1-f_c)(1+F_{n_{ab}})$ |

One can show that (7) corresponds to an effective wave equation which is given by

$$(E_a+E_b-z)\Psi_{P\nu}(p_ap_b,rt)+[1-f_a(p_a,r,t)-f_b(p_b,r,t)]$$
$$\times\int\frac{d^3\bar{p}_a\,d^3\bar{p}_b}{(2\pi\hbar)^3}V(p_a-\bar{p}_a)\delta(P-\bar{P})\Psi_{P\nu}(\bar{p}_a\bar{p}_b,rt). \quad (9)$$

This wave equation determines the two-particle states $\Psi_{P\nu}(p_ap_b)=\langle p_ap_b|\nu P\rangle$ taking into account medium effects. There are the following types of solutions:

$$|\nu P\rangle=\begin{cases}|Pj\rangle, & \text{bound states,}\\ |Pp+\rangle, & \text{scattering states,}\end{cases}$$

where $P=p_a+p_b$ and $p=(m_bp_a-m_ap_b)/(m_a+m_b)$ are the total and relative momenta, respectively. The three-particle collision processes are described by the $T$ operators

$$T^{\kappa\kappa'}_{abc}=V^{\kappa}_{abc}+i^2V^{\kappa}_{abc}\frac{N_{abc}}{z-H^{0\,\mathrm{eff}}_{abc}-N_{abc}V^0_{abc}}V^{\kappa'}_{abc}, \quad (10)$$

which determine the transition probabilities between the initial and the final three-body scattering channels. Here $H^{0\,\mathrm{eff}}_{abc}$ denotes the Hamiltonian of three free quasiparticles with the single-particle energies given by (3). Further, we have in first order, with respect to phase space occupation,

$$N_{abc}=1-f_a-f_b-f_c,$$
$$V^0_{abc}=(1+f_c)V_{ab}+(1+f_b)V_{ac}+(1+f_a)V_{bc}, \quad (11)$$
$$V^1_{abc}=(1+f_b)V_{ac}+(1+f_c)V_{ab}, \quad \text{etc.}$$

In addition to the kinetic equation (2), an equation can be derived for the distribution functions $F_j$ of the bound particles. On the lhs of this equation, the quasiparticle energies of the bound states appear, and the rhs accounts for the collisions between the bound and the free particles. The explicit expression for the three-particle collision term, being similar to that of (6), can be found in.[18]

## III. MANY-BODY EFFECTS IN DENSE PLASMAS

In the following, we consider a strongly coupled plasma consisting of electrons, singly charged ions, and atoms in the state $|j\rangle$, where $j$ denotes the set of internal quantum numbers. The number densities are $n_e$, $n_i$, and $n_j$, respectively. It is well known that the properties of strongly coupled plasmas are essentially determined by those many-body effects that were discussed in the previous section. Additionally, the screening of the long-ranged *Coulomb* interaction must be taken into account. This can be done replacing the Coulomb potential by a screened one which can be written as

$$V^s_{ab}(qz,rt)=\frac{V_{ab}(q)}{\epsilon(qz,rt)}. \quad (12)$$

Here $V_{ab}=4\pi e^2/q^2$ is the Coulomb potential, and $\epsilon(qz,rt)$ is the dielectric function

$$\epsilon(qz,rt)=1-\sum_a V_{aa}\Pi_{aa}(qz,rt). \quad (13)$$

The latter is given in terms of the polarization function $\Pi_{aa}(qz,rt)$, which can be determined using the techniques of quantum statistical theory of charged particle systems.

In the $V^s$ approximation and if local equilibrium is assumed, the single-particle energy shift in (3) is given by[6]

$$\mathrm{Re}\,\Sigma^R_a(p\omega,rt)=\int\frac{d^3q}{(2\pi)^3}V_{aa}\Bigg(f_a(\mathbf{p}+\mathbf{q},rt)$$
$$+P\int_{-\infty}^{\infty}\frac{d\omega}{2\pi}\,\mathrm{Im}\,\varepsilon^{-1}(q\omega,rt)$$
$$\times\frac{1-f_a(\mathbf{p}+\mathbf{q},rt)-n_B(\omega)}{z-\omega-E_a(\mathbf{p}+\mathbf{q},rt)}\Bigg), \quad (14)$$

with $n_B(\omega)=(e^{\beta\omega}-1)^{-1}$.

To work with the energy shifts given by (14) is difficult. A possible approximation is to use thermally averaged shifts in the framework of the "rigid shift" approximation.[19] In this case, the energy shift is replaced by a momentum-independent shift reproducing the correct normalization (the correct density $n_a$). If local equilibrium is assumed, we have

$$\Delta_a(r,t)=\frac{\int d^3p\,\mathrm{Re}\,\Sigma^R_a(p,r,t)(\partial/\partial\mu^{\mathrm{id}}_a)f_a(p,r,t)}{\int d^3p(\partial/\partial\mu^{\mathrm{id}}_a)f_a(p,r,t)}. \quad (15)$$

It can be shown that the thermally averaged shift is related to the chemical potential by

$$\mu_a=\mu^{\mathrm{id}}_a+\Delta_a, \quad (16)$$

that means, $\Delta_a$ is equal to the interaction part of the chemical potential. In the nondegenerate case and if we assume in (14) the static approximation, we obtain in lowest order $(a=e,i)$

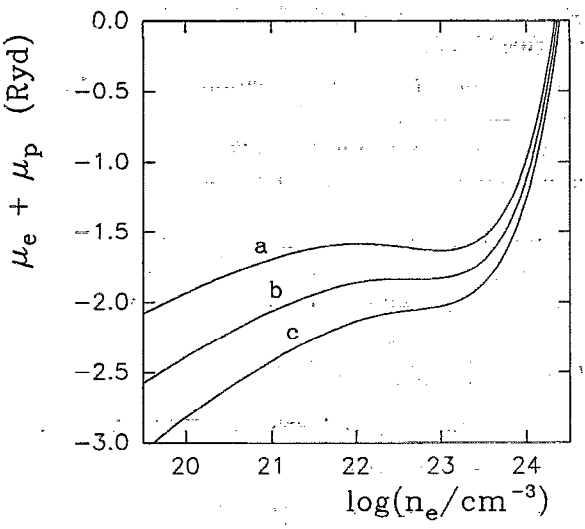

FIG. 2. Isotherms of the plasma chemical potential $\mu_e+\mu_p$ for hydrogen versus free electron density. The expressions for the correlation contributions of the electron and proton chemical potentials are given in the Appendix. The temperatures are (a) $T=14\,000$ K, (b) 17 000 K, and (c) 20 000 K.

$$\Delta_a=-\frac{\kappa e^2}{2}, \quad \kappa^2=\frac{4\pi\Sigma_a(n_a e_a^2)}{k_BT}. \tag{17}$$

This is the Debye shift which represents the limiting law for systems with Coulomb interactions. In a first approximation, it describes the influence of the plasma medium on the single-particle properties.

In general, one has to carry out quantum statistical calculations in order to obtain better results for the one-particle shifts. We have applied the two-fluid model which results in an electron and an ion gas contribution including the Hartree–Fock and Montroll–Ward terms in the exchange correlation part of the plasma chemical potential. In Fig. 2, the chemical potential of the free charged particles for a hydrogen plasma is shown that was calculated on the basis of Padé interpolation formulas (cf., e.g., Ref. 20) given in the Appendix. An interesting feature is the "van der Waals loop" which is, in equilibrium, connected with the plasma phase transition.[21,22] As we will show, this property has important consequences in nonequilibrium situations, too.

The main result of the many-body effects in dense plasmas is the lowering of the ionization energy of the two-particle bound states. Therefore, the properties of the two-particle states in plasmas are of special importance in order to describe the macroscopic behavior of dense nonideal plasmas. An effective wave equation for the two-particle states in a dense plasma can be derived on the basis of Green's function techniques. In $V^s$ approximation, one obtains instead of (9)[23–25]

$$\begin{aligned}&[\varepsilon_a(p_a)+\varepsilon_b(p_b)+\Delta_{12}^{\mathrm{eff}}(p_ap_bz)-z]\Psi(p_ap_b)\\&\quad-[1-f_a(p_a)-f_b(p_b)]\\&\quad\times\int V^{\mathrm{eff}}(p_ap_bqz)\Psi(p_a+q,p_b-q)d^3q=0,\end{aligned} \tag{18}$$

where $\varepsilon_a(p_a)=p_a^2/2m_a$, $a=e,i$.

One can see that, in comparison with the Schrödinger equation of an isolated pair of particles, there are some differences arising from the inclusion of many-body effects. The latter are condensed in the self-energy corrections, Pauli blocking, and in the effective potential. The modifications, in comparison with the effective wave equation (9) given in the previous section, are based on the inclusion of special plasma effects like dynamical screening. If we consider the nondegenerate case, the dynamically screened effective potential is given by

$$\begin{aligned}&V_{ab}^{\mathrm{eff}}(p_ap_bqz)-V_{ab}(q)\\&\quad=V_{ab}(q)\int_{-\infty}^{\infty}\frac{d\omega}{\pi}\,\mathrm{Im}\,\epsilon^{-1}(q,\omega+i0)\\&\quad\times\left(\frac{n_B(\omega)+1}{z-\omega-\varepsilon_a(p_a)-\varepsilon_b(p_b-q)}\right.\\&\quad\left.+\frac{n_B(\omega)+1}{z-\omega-\varepsilon_a(p_a+q)-\varepsilon_b(p_b)}\right),\end{aligned} \tag{19}$$

and we obtain for the dynamical self-energy

$$\Delta_{ab}^{\mathrm{eff}}(p_ap_bz)=\int\frac{d^3q}{(2\pi\hbar)^3}\,[V_{ab}^{\mathrm{eff}}(p_ap_bqz)-V_{ab}(q)]. \tag{20}$$

In the static limit, the effective potential simplifies to

$$V_{ab}^{\mathrm{eff}}(p_ap_bq,0)=\frac{V_{ab}(q)}{\epsilon(q,0)}, \quad \epsilon(q,0)=\left(\frac{q^2}{q^2+\kappa^2}\right)^{-1},$$

which is the statically screened Debye potential. For the thermally averaged two-particle energy shifts, we obtain with (17)

$$\Delta_{ab}^{\mathrm{eff}}=\Delta_a+\Delta_b=-\kappa e^2.$$

Two problems can be solved with the effective wave equation (18). First, the two-particle bound and scattering states can be determined accounting for the influence of many-body effects. Furthermore, the influence of the surrounding plasma on the two-particle energy spectrum is described. In order to show that, we apply perturbation theory as a first step. The wave equation (18) is written for this purpose in the following form:

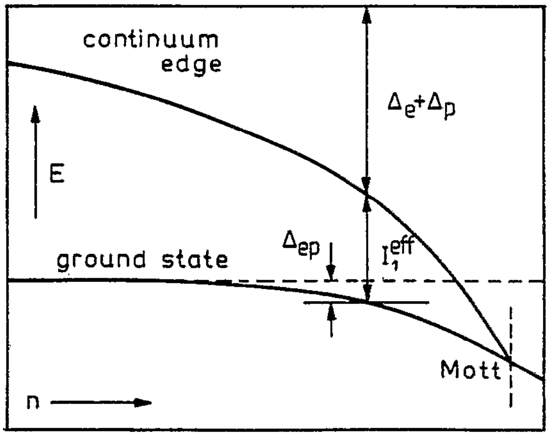

FIG. 3. Density dependence of the continuum edge and the ground state level for hydrogen (qualitatively). Here $I_1^{\mathrm{eff}}$ denotes the effective ionization energy vanishing at the crossing point (Mott density).

$$(H_{ab}^0-E_{\nu P})\,|\alpha P\rangle=-H_{ab}^{pl}(E_{\nu P})\,|\alpha P\rangle, \tag{21}$$

where $H_{ab}^0$ is the Hamiltonian of the isolated two-particle problem and $H_{ab}^{pl}$ includes all the many-body effects discussed above. The explicit expression for $H_{ab}^{pl}$ follows from (18) with (19) and (20). In first-order perturbation theory with respect to $H_{ab}^{pl}$, we find for the discrete two-particle energies

$$E_{jP}=E_{jP}^0+\mathrm{Re}\langle jP|H_{ab}^{pl}(E_j^0)\,|jP\rangle,$$

and for the scattering energies

$$E_{pP}=\frac{p^2}{2m_{ab}}+\frac{P^2}{2(m_a+m_b)}+\Delta_{ab}^{\mathrm{eff}},$$

where $m_{ab}$ denotes the reduced mass. The result of the numerical evaluation for the case of the ground state energy ($j=1$) of atomic hydrogen is given in Fig. 3.

(i) We observe a lowering of the ionization energy $I_1^{\mathrm{eff}}=|E_1|-\Delta_{ep}^{\mathrm{eff}}+\Delta_1$ with increasing plasma density which follows mainly from the lowering of the continuum edge.

(ii) There is a crossover of the continuum edge and the ground state energy at high densities that defines the so-called Mott density. Bound states do not exist above this density. The disappearance of bound states is referred to as the Mott effect.

## IV. THE COEFFICIENTS OF IONIZATION AND RECOMBINATION

Now we apply the kinetic equations given in Sec. II to a strongly coupled plasma including the many-body effects discussed above. As in the previous section, we consider the plasma consisting of electrons, ions, and atoms in the state $|j\rangle$.

In order to describe the macroscopic properties of the plasma, we introduce macroscopic observables in the usual way. We define the number density of species $a$ by

$$n_a(\mathbf{r},t)=\int\frac{d^3p}{(2\pi\hbar)^3}f_a(\mathbf{p},\mathbf{r},t). \tag{22}$$

The diffusion current $\mathbf{j}_a^D(\mathbf{r},t)$ can be written in the form

$$\mathbf{j}_a^D=n_a\mathbf{w}_a=n_a(\mathbf{u}_a-\mathbf{u}), \tag{23}$$

where the mean velocity $\mathbf{u}_a$ is given by

$$n_a(\mathbf{r},t)\mathbf{u}_a(\mathbf{r},t)=\int\frac{d^3p}{(2\pi\hbar)^3}\frac{\partial E_a(\mathbf{p},\mathbf{r}t)}{\partial\mathbf{p}}f_a(\mathbf{p},\mathbf{r},t) \tag{24}$$

and the mass average velocity $\mathbf{u}$ by

$$\mathbf{u}=\frac{1}{\rho}\sum_a\rho_a\mathbf{u}_a,$$

with $\rho=\Sigma_a\rho_a$ and $\rho_a=n_am_a$ being the mass density of species $a$. For the free charged particles, the species index is $a=e,i$ and for the atoms in the state $|j\rangle$ we write $a=j$.

Equations governing the evolution of the number densities in space and time can be obtained by integrating the kinetic equations with respect to the corresponding momentum. The result is

$$\frac{\partial}{\partial t}n_a(\mathbf{r},t)+\mathrm{div}\,j_a^D(\mathbf{r},t)=W_a(\mathbf{r},t)-\mathrm{div}[n_a(\mathbf{r},t)\mathbf{u}(\mathbf{r},t)], \tag{25}$$

where $W_a$ is the source function that describes the change of $n_a(\mathbf{r},t)$ because of ionization and recombination processes in the plasma. The explicit form of $W_a$ follows from the rhs of the kinetic equations, especially from the reaction terms in the three-particle collision integrals. In Eq. (25), for the electron density, the source function can be written in the form

$$W_e=\sum_{c=e,i}\sum_j(\alpha_c^jn_cn_j-\beta_c^jn_cn_en_i), \tag{26}$$

and it follows $W_e=W_i=-\Sigma_jW_j$.

In (26), we have introduced the coefficients of impact ionization and three-body recombination of the atomic level $j$. If degeneracy effects are neglected, one obtains[12,26–28]

$$\alpha_j=\frac{1}{\hbar V}\sum_{a=e,i}\int\frac{d^3P}{(2\pi\hbar)^3}\frac{d^3p_a}{(2\pi\hbar)^3}\frac{d^3\bar{P}}{(2\pi\hbar)^3}\frac{d^3\bar{p}}{(2\pi\hbar)^3}\frac{d^3\bar{p}_a}{(2\pi\hbar)^3}2\pi\delta(E_{123}^3-\bar{E}_{123}^0)\,|\langle jP|\langle p_a|T_{123}^{33}(E_{123}^3+i\varepsilon)\,|\bar{p}_a\rangle\,|\bar{P}\bar{p}+\rangle\,|^2\frac{f_a}{n_a}\frac{F_j}{n_j}, \tag{27}$$

$$\beta_j=\frac{1}{\hbar V}\sum_{a=e,i}\int\frac{d^3P}{(2\pi\hbar)^3}\frac{d^3p_a}{(2\pi\hbar)^3}\frac{d^3\bar{P}}{(2\pi\hbar)^3}\frac{d^3\bar{p}}{(2\pi\hbar)^3}\frac{d^3\bar{p}_a}{(2\pi\hbar)^3}2\pi\delta(E_{123}^3-\bar{E}_{123}^0)\,|\langle jP|\langle p_a|T_{123}^{33}(E_{123}^3+i\varepsilon)\,|\bar{p}_a\rangle\,|\bar{P}\bar{p}+\rangle\,|^2\frac{\bar{f}_a}{n_a}\frac{\bar{f}_e}{n_e}\frac{\bar{f}_i}{n_i}. \tag{28}$$

Let us now consider the problem of the calculation of these rate coefficients. A considerable simplification is possible if we take into account that there are different time scales during the approach to thermodynamic equilibrium. First, the system comes into equilibrium with respect to the translational degrees of freedom and then with respect to those of internal ones. At the latest stage, the chemical equilibrium is established. In the following, we will assume that local equilibrium has been reached already, so that the results being valid for equilibrium situations can be used. In the nondegenerate case, we have for the distribution functions of the free charged particles

$$f_a^0(\mathbf{p},\mathbf{r},t)=\exp\{-\beta[E_a(\mathbf{p},\mathbf{r},t)-\mu_a(\mathbf{r},t)]\} \tag{29}$$

and for the bound particles in the state $|j\rangle$

$$F_j^0(\mathbf{P},\mathbf{r},t)=\exp\{-\beta[E_j(\mathbf{P},\mathbf{r},t)-\mu_j(\mathbf{r},t)]\}. \tag{30}$$

Here, $E_a(\mathbf{p},\mathbf{r},t)$ and $E_j(\mathbf{P},\mathbf{r},t)$ are the quasiparticle energies, and $\mu_a(\mathbf{r},t)$ and $\mu_j(\mathbf{r},t)$ are the chemical potentials of the free and bound particles, respectively. We keep in mind that ionization equilibrium has not been established yet, that means

$$\mu_e(\mathbf{r},t)+\mu_i(\mathbf{r},t)\neq\mu_j(\mathbf{r},t).$$

In the approximation of thermally averaged shifts (15), it is easy to derive the following simple relation between the rate coefficients:

$$\beta_j=\alpha_j\Lambda_e^3\exp[-(E_j^0+\Delta_j-\Delta_e-\Delta_i)/k_BT]. \tag{31}$$

In the case of ionization equilibrium, we arrive, therefore, at

$$n_j/n_en_i=\Lambda_e^3\exp[-(E_j^0+\Delta_j-\Delta_e-\Delta_i)/k_BT]. \tag{32}$$

This is the well-known Saha equation for a nonideal plasma. The nonideality is contained in the energy shifts of the particles leading to a lowering of the ionization energy $\Delta I_j$ given by

$$I_j^{\text{eff}}=|E_j^0|-\Delta I_j,\quad \Delta I_j=\Delta_j-\Delta_e-\Delta_i. \tag{33}$$

Let us come back to situations where chemical equilibrium has not been reached yet. Because of (31), it is sufficient to calculate explicitly only one of the rate coefficients. In the nondegenerate case, the ionization coefficient for electron impact can be written in the following form:

$$\alpha_j=\frac{8\pi m_e}{(2\pi m_ek_BT)^{3/2}}\int_{I_j^{\text{eff}}}^{\infty}d\varepsilon\,\varepsilon\sigma_j^{\text{ion}}(\varepsilon)e^{-\beta\varepsilon},\quad \varepsilon=\frac{p^2}{2m_e}, \tag{34}$$

where $\sigma_j^{\text{ion}}$ is the impact ionization cross section from the atomic state $|j\rangle$ which reads, in statically screened first Born approximation,

$$\sigma_j^{\text{ion}}=\frac{8\pi\hbar^2}{p_e^2a_{\text{B}}^2}\int_0^{\bar{p}_{\max}}d\bar{p}\,\bar{p}^2\,d\Omega_{\bar{p}}\int_{q_{\min}}^{q_{\max}}q\,dq\,|V_{ee}^{\text{eff}}(q)P_{j\mathbf{p}}(q)|^2. \tag{35}$$

Here $\hbar\mathbf{q}=\mathbf{p}_e-\bar{\mathbf{p}}_e$ denotes the momentum transfer of the projectile, and

$$\bar{p}_{\max}=(p_e^2-2m_eI^{\text{eff}})^{1/2},$$

$$\bar{p}_e=(p_e^2-2m_eI^{\text{eff}}-\bar{p}^2)^{1/2},$$

$$\hbar q_{\min}=p_e-\bar{p}_e,$$

$$\hbar q_{\max}=p_e+\bar{p}_e,$$

follow from energy conservation. The effective ionization energy $I_j^{\text{eff}}$ is given by (33). With $P_{j\bar{p}}$, we denote the atomic form factor

$$P_{j\mathbf{p}}(q)=\int d^3r\,\Psi_j^*(\mathbf{r})\Psi_{\mathbf{p}}^+(\mathbf{r})e^{(i/\hbar)\mathbf{q}\cdot\mathbf{r}}. \tag{36}$$

The two-particle wave functions $\Psi_j(\mathbf{r})$ for the atomic bound states and $\Psi_{\bar{p}}^+(\mathbf{r})$ for the scattering states have to be determined from the effective wave equation (18).

The simplest approximation for $\sigma_j$ follows if we restrict ourselves to ground state ionization ($j=1$) and if we use for $V_{ee}^{\text{eff}}$ the Coulomb potential and for the wave functions the Coulombic ones. In this case, many-body effects are taken into account by energy shifts only. Then, the following modified Bethe formula is a good approximation:[26,27]

$$\sigma_1^{\text{ion}}=2.5\pi a_{\text{B}}^2\frac{|E_1^0|}{\varepsilon}\ln\frac{\varepsilon-\Delta_e-\Delta_p+\Delta_1}{|E_1|}. \tag{37}$$

Inserting (37) in (34), the following interesting and simple expression can be derived:

$$\alpha_1=\alpha_1^{\text{id}}e^{(\Delta_1-\Delta_e-\Delta_p)/k_BT},$$

$$\alpha_1^{\text{id}}=\frac{10\pi a_{\text{B}}^2E_1}{(2\pi m_ek_BT)^{3/2}}Ei\left(-\frac{|E_1^0|}{k_BT}\right), \tag{38}$$

with $Ei(x)=\int_{-\infty}^{x}(e^t/t)dt$.

Expression (38) for the ionization coefficient represents a generalization to a strongly coupled plasma. We have the usual ideal part and an additional contribution in terms of energy shifts following from the inclusion of the many-particle effects in the plasma. Using (38) in (31), we obtain for the recombination coefficient

$$\beta=\beta^{\text{id}}.$$

That means $\beta$ remains density independent in this first approximation. More general results for the impact ionization and three-body recombination coefficient are given in Ref. 18 taking into account energy shifts, effective potentials, and Pauli-blocking.

In Fig. 4, the results for $\alpha_1$ are shown following from (38) for a hydrogen plasma. The most important result is the strong nonlinear density dependence of the ionization coefficient which is a direct consequence of the nonideality effects condensed in the quasiparticle energy shifts.

## V. NONLINEAR DIFFUSION

In order to obtain a closed system of equations for the number densities, we have to determine the diffusion current density given by (23). For this purpose, we multiply each of the kinetic equations (2) by the corresponding

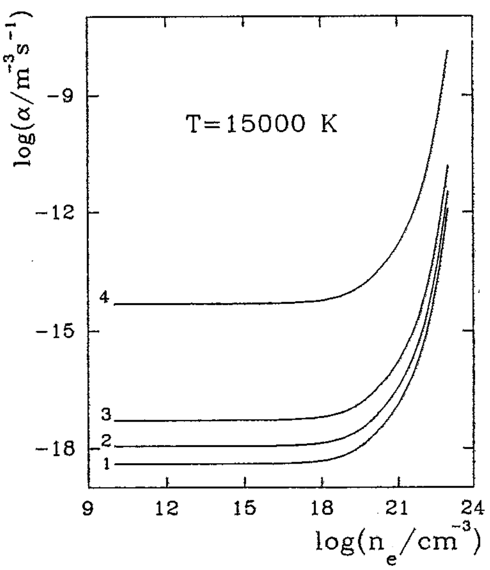

FIG. 4. Ionization coefficient of a nonideal hydrogen plasma. For the energy shifts of the free and bound particles, the correlation parts of the chemical potential given in the Appendix were used. The values of the density of atoms $n_H$ are (in cm$^{-3}$): (1) $10^{21}$, (2) $5\times10^{22}$, (3) $10^{23}$, and (4) $2\times10^{23}$.

momentum and integrate with respect to the latter. We obtain the following equation of motion for the mean velocity:[28–30]

$$\rho_a \frac{D_a}{Dt} u_{ai} - \frac{\partial}{\partial r_j} \rho_a u_{ai} u_{aj} + \frac{\partial}{\partial r_j} \Pi_{aij} = S_{ai} \qquad (39)$$

with

$$\frac{D_a}{Dt} = \frac{\partial}{\partial t} + u_{aj} \frac{\partial}{\partial r_j}.$$

The rhs accounts for the influence of collisions on the momentum balance of species $a$. It is given by

$$\mathbf{S}_a = \mathbf{R}_a - \mathbf{u}_a m_a W_a$$

with

$$\mathbf{R}_a(\mathbf{r},t) = \sum_b \int \frac{d^3 p_a}{(2\pi\hbar)^3} \mathbf{p}_a I_{ab}(\mathbf{p}_a,\mathbf{r},t) + \sum_{bc} \int \frac{d^3 p_a}{(2\pi\hbar)^3} \mathbf{p}_a I_{abc}(\mathbf{p}_a,\mathbf{r},t).$$

The pressure tensor on the lhs of (39) is defined by the relation

$$\frac{\partial}{\partial r_j} \Pi_{aij} = \frac{\partial}{\partial r_j} \int \frac{d^3 p_a}{(2\pi\hbar)^3} p_{ai} \frac{\partial E_a}{\partial p_{aj}} f_a + \int \frac{d^3 p_a}{(2\pi\hbar)^3} \frac{\partial E_a}{\partial r_j} f_a \delta_{ij}. \qquad (40)$$

The pressure tensor for the bound states follows if the binding energies $E_j$ are used and if the distribution functions $f_a$ are replaced by the $F_j$'s. It should be mentioned again that the $E_a = E_a(p_a,r,t)$ are quasiparticle energies given by (3). Therefore, the expression (40) is an important generalization of the ideal gas result because it contains nonideality contributions in terms of energy shifts.

The equation of motion for the mass-averaged velocity can be obtained from (39) by summation over the species:

$$\rho \frac{D}{Dt} u_i - \frac{\partial}{\partial r_j} \rho u_i u_j + \frac{\partial}{\partial r_j} \sum_a \Pi_{aij} = 0 \qquad (41)$$

with

$$\frac{D}{Dt} = \frac{\partial}{\partial t} + u_j \frac{\partial}{\partial r_j}.$$

In the following, the system is assumed to be in a stage where local equilibrium is established only for each plasma species. In the approximation of thermally averaged shifts and assuming

$$w_a \ll v_a^T = (k_B T/m_a)^{1/2},$$

the distribution function can be used in the form[31]

$$f_a = f_a^0 \left( 1 + \frac{\mathbf{c}_a \cdot \mathbf{w}_a}{k_B T} \right), \quad \mathbf{c}_a = \mathbf{p}_a - m_a \mathbf{u} \qquad (42)$$

with the notation

$$f_a^0(p_a,r,t) = n_a \Lambda_a^3 \exp\left( -\frac{(\mathbf{p}_a - m_a \mathbf{u})^2}{2 m_a k_B T} \right).$$

A similar expression follows for the distribution function $F_j$ of the bound states.

Neglecting contributions nonlinear in $\mathbf{u}$, we simplify (41) to

$$\rho \frac{\partial}{\partial t} \mathbf{u} \approx -\nabla P.$$

Inserting this result in the equation of motion (39), we obtain

$$\nabla p_a - \frac{\rho_a}{\rho} \nabla P = \mathbf{R}_a - m_a \mathbf{u}_a W_a = \mathbf{S}_a, \qquad (43)$$

where we can write

$$\frac{\partial}{\partial r_j} \Pi_{aij} = \nabla p_a \delta_{ij}.$$

According to (40) and using momentum-independent shifts, the pressure gradients are given by

$$\nabla P(\mathbf{r},t) = \nabla \sum_a p_a(\mathbf{r},t), \qquad (44)$$

$$\nabla p_a(\mathbf{r},t) = \nabla p_a^{\mathrm{id}}(\mathbf{r},t) + n_a \nabla \Delta_a(\mathbf{r},t). \qquad (45)$$

It should be mentioned here that the $p_a$ cannot be considered as pure partial pressures because of the interaction between the different plasma components taken into account in the shifts $\Delta_a$.

Equation (43) connects the thermodynamic forces of the nonideal plasma with the momentum transfer due to the collision processes. In a first step, we will restrict ourselves to elastic scattering contributions ($S_a = R_a^{\mathrm{el}}$). The rhs of Eqs. (39) and (43) can be expressed then in terms of the diffusion currents

$$\mathbf{S}_a=\mathbf{R}_a^{\mathrm{el}}=\sum_b \frac{k_BT}{n\mathscr{D}_{ab}}(n_a\mathbf{j}_b^D-n_b\mathbf{j}_a^D), \tag{46}$$

where $n$ is the total number density. In (46), the binary diffusion coefficients were introduced:

$$\mathscr{D}_{ab}^{-1}=n\frac{8}{3\sqrt{\pi}}\left(\frac{2m_{ab}}{k_BT}\right)^{1/2}\int_0^\infty z^5e^{-z^2}Q_{ab}^T(z)dz. \tag{47}$$

Here we have $z^2=(\mathbf{p}_a-\mathbf{p}_b)^2/2m_{ab}$, $m_{ab}=m_am_b/(m_a+m_b)$ is the reduced mass, and $Q_{ab}^T$ is the transport cross section given by

$$Q_{ab}^T=2\pi\int_0^\pi d\Theta \sin\Theta(1-\cos\Theta)\sigma_{ab} \tag{48}$$

with $\sigma_{ab}$ being the differential scattering cross section.

Equation (43) with expression (46) for the diffusion currents can be solved in the standard way. The result is

$$\mathbf{j}_a^D=\frac{n}{\rho k_BT}\sum_{b\neq a} m_bD_{ab}\left(\nabla p_b-\frac{\rho_b}{\rho}\nabla p\right), \tag{49}$$

where $\Sigma_a\mathbf{R}_a^{\mathrm{el}}=0$ and $\Sigma_am_a\mathbf{j}_a^D=0$ was used; $D_{ab}$ are the multicomponent diffusion coefficients that can be expressed in terms of the binary diffusion coefficients.

In the following, the atoms in the plasma are assumed to be in the ground state only ($j=1$). Then we have a three-component plasma, and the $D_{ab}$ can be written as

$$D_{ab}=\mathscr{D}_{ab}\left(1+\frac{n_c[\mathscr{D}_{ac}(m_c/m_b)-\mathscr{D}_{ab}]}{n_a\mathscr{D}_{ab}+n_b\mathscr{D}_{ac}+n_c\mathscr{D}_{ab}}\right). \tag{50}$$

Inserting (49) into the balance equation (25) for the number density, we find for the free charged particles

$$\frac{\partial}{\partial t}n_a+\mathrm{div}(n_a\mathbf{u})+\mathrm{div}\left[\frac{n}{k_BT\rho}\sum_{b\neq a}D_{ab}\left(\nabla p_b-\frac{\rho_b}{\rho}\nabla P\right)\right]$$

$$=\sum_{c=e,i}(\alpha_c^1n_cn_1-\beta_c^1n_cn_en_i) \tag{51}$$

and for the atoms

$$\frac{\partial}{\partial t}n_1+\mathrm{div}(n_1\mathbf{u})+\mathrm{div}\left[\frac{n}{k_BT\rho}\sum_{b\neq 1}D_{1b}\left(\nabla p_b-\frac{\rho_b}{\rho}\nabla P\right)\right]$$

$$=\sum_{c=e,i}(\beta_c^1n_cn_en_i-\alpha_c^1n_cn_1). \tag{52}$$

These equations represent a system of reaction-diffusion equations for a nonideal plasma. Many-body effects are included in the diffusion terms as well as in the ionization and recombination rates. The latter were discussed in the previous section.

Before we turn to further investigation of Eqs. (51) and (52), we have to make sure that our theory (with all assumptions made) leads to results that are thermodynamically consistent. As it was shown, nonideality is taken into account in the quasiparticle picture by energy shifts according to (3). Approximating the latter by momentum-independent energy shifts, we cannot, of course, reproduce completely the nonequilibrium properties. But in our case it is sufficient to calculate density, chemical potential, and the gradients of the scalar pressures in a consistent way. This is indeed possible. The definition of the shifts $\Delta_a$ in (15) and (16) leads to a correct result for the number density $n_a$ and provides the chemical potential with $\mu_a^{\mathrm{int}}=\Delta_a$. Let us consider the definition of the pressure tensor. The first term on the rhs of (40) gives the ideal pressure, the second one the nonideality corrections. The result for the pressure gradient was given above by (44) and (45). The basic thermodynamic equation we have to deal with is the Gibbs–Duhem relation:

$$dP=\sum_a n_a\,d\mu_a, \quad \text{for} \quad T=\text{const}. \tag{53}$$

Of course it is fulfilled for the ideal parts of pressure and chemical potential. If (45) is inserted in (44), the second term has to coincide with

$$\sum_a n_a\,d\mu_a^{\mathrm{int}},$$

what in fact is the case because of the connection (16) between chemical potential and thermally averaged energy shift.

Let us now study in more detail the diffusion process in a nonideal three-component plasma. If, in the diffusion process, electrons and ions separate, an electrical field will be set up acting like an additional thermodynamic force. This leads to a steady state with charge neutrality and equal electron and ion number fluxes (ambipolar diffusion)

$$n_e(r,t)=n_i(r,t), \quad j_e^D(r,t)=j_i^D(r,t).$$

Further we suppose $\nabla p\approx 0$. With $u\approx 0$, we have $n=n_e+n_1=\text{const}$, and the system of reaction-diffusion equations (51) and (52) reduces to only one equation which reads

$$\frac{\partial}{\partial t}n_e(r,t)+\mathrm{div}\,\mathbf{j}_e^D(r,t)=\sum_{c=e,i}(\alpha_c^1n_cn_1-\beta_c^1n_cn_en_i). \tag{54}$$

The diffusion current density can be written as

$$\mathbf{j}_e^D=-D_{\mathrm{AMB}}^0\frac{n_e}{k_BT}\left(\frac{\partial}{\partial n_e}+\frac{\partial}{\partial n_i}\right)(\mu_e+\mu_i)\nabla n_e, \tag{55}$$

where $D_{\mathrm{AMB}}^0$ is the usual ambipolar diffusion coefficient[28,32]

$$D_{\mathrm{AMB}}^0=\frac{n}{\rho}\frac{m_iD_{ei}m_AD_{iA}+m_eD_{ie}m_AD_{eA}-m_eD_{ie}m_iD_{ei}}{m_eD_{ie}+m_iD_{ei}}. \tag{56}$$

In deriving (55) the interaction between charged and neutral particles was neglected in the energy shifts $\Delta_e$ and $\Delta_i$. In this approximation, the shifts depend on the charged particle density only. We can interpret the total prefactor of $\nabla n_e$ in (55) as a nonideal ambipolar diffusion coefficient

$$D_{\mathrm{AMB}}=D_{\mathrm{AMB}}^0\frac{n_e}{k_BT}\left(\frac{\partial}{\partial n_e}+\frac{\partial}{\partial n_i}\right)(\mu_e+\mu_i). \tag{57}$$

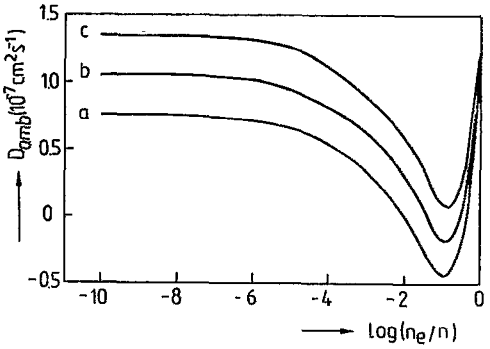

FIG. 5. Ambipolar diffusion coefficient for hydrogen versus the degree of ionization $c=n_e/(n_e+n_H)$ for different temperature values: (a) $T=10\,000$ K, (b) 14 000 K, and (c) 18 000 K. The total density is constant $n=5\times10^{23}$ cm$^{-3}$.

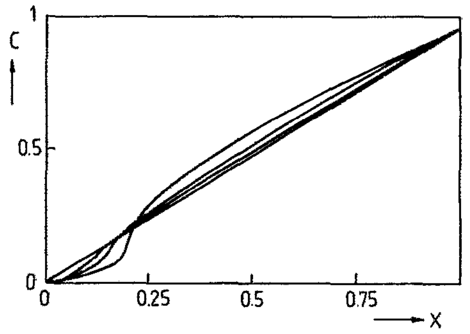

FIG. 6. Solution of the nonlinear diffusion equation with the density-dependent diffusion coefficient $D_{\mathrm{AMB}}(c)$ (58) for Dirichlet boundary conditions, $T=18\,000$ K, $n=3\times10^{23}$ cm$^{-3}$. Here $x$ is the dimensionless length, scaled by the system length $L$. The straight line is the initial profile, the steplike one represents the asymptotic (stationary) distribution. The inner curves correspond to the dimensionless time 0.006 and 0.0156, respectively. The time unit is $t_0=L^2/D^0_{\mathrm{AMB}}$.

A density-dependent diffusion coefficient can be introduced formally in this way which describes nonlinear diffusion due to many-body effects.

For demonstration, we again consider a hydrogen plasma. The calculation of the binary diffusion coefficients (47) entering the coefficients $D_{ab}$ first requires one to determine the corresponding transport cross sections given by (48). In the case of the electron–proton collisions, the scattering phase shifts were calculated by numerical solution of Schrödinger's equation adopting the statically screened Debye potential. The elastic scattering of electrons on hydrogen atoms in the ground state was treated using the adiabatic exchange model taking into account a statically screened polarization potential. The cross section of the proton–atom scattering was calculated classically. The result for the usual ambipolar diffusion coefficient $D^0_{\mathrm{AMB}}$ is that the proton–atom scattering gives the dominating contribution for arbitrary plasma composition in the whole density range,[32] that means

$$D^0_{\mathrm{AMB}}\approx\mathscr{D}_{pH}\,.$$

Then, the ambipolar diffusion coefficient for the nonideal hydrogen plasma can be written as

$$D_{\mathrm{AMB}}=\mathscr{D}_{pH}\frac{n_e}{k_BT}\left(\frac{\partial}{\partial n_e}+\frac{\partial}{\partial n_i}\right)(\mu_e+\mu_p),\qquad(58)$$

where the chemical potentials are given by $(a=e,p)$

$$\mu_a=\mu_a^{\mathrm{id}}+\mu_a^{\mathrm{int}},\quad \mu_a^{\mathrm{int}}=\Delta_a\,.$$

For $\mu_a^{\mathrm{int}}$, we used the same expressions (cf. the Appendix) as presented in Fig. 2. The isotherms of the nonideal ambipolar diffusion coefficient $D_{\mathrm{AMB}}$ are shown in Fig. 5. The classical result $D_{\mathrm{AMB}}=2\mathscr{D}_{pH}$ occurs only for electron densities below $10^{15}$ cm$^{-3}$. For higher densities, the many-body effects cause a minimum and, below $T=17\,000$ K, even negative values of $D_{\mathrm{AMB}}$ are a direct consequence of the "van der Waals loop" in the plasma chemical potential (cf. Fig. 2).

Obviously, the diffusion of particles in a region of high electron density will differ from that at low concentration. This can be seen considering the nonlinear diffusion equation neglecting for a moment the reaction term in (54). The stationary solution in the one-dimensional case can be written immediately $(c=n_e/n)$, $x$ being a dimensionless length $(0\leqslant x\leqslant 1)$:

$$x(c)=\frac{\int_{c(0)}^{c}D_{\mathrm{AMB}}(c',n,\tau)dc'}{\int_{c(0)}^{c(1)}D_{\mathrm{AMB}}(c,n,\tau)dc}\,.$$

For $D_{\mathrm{AMB}}>0$, the profile is always monotonous. However, the curvature can change the sign because $d^2x(c)/dc^2\sim dD_{\mathrm{AMB}}/dc$. Because of the minimum of $D_{\mathrm{AMB}}$, the stationary profile is of steplike shape. This can be seen from Fig. 6 where the nonlinear diffusion equation was solved numerically starting with a linear concentration profile [Dirichlet boundary conditions $c(0)=c_1$, $c(1)=c_2$] which is the stationary solution in the case of constant diffusion $D_{\mathrm{AMB}}=$const. If we could "switch on" the nonlinearity in the diffusion coefficient at $t=0$, we would see exactly the evolution shown in Fig. 6.[32]

## VI. NONIDEALITY AND NONLINEAR IONIZATION KINETICS IN DENSE PLASMAS

Because of nonideality, the source function in the reaction-diffusion equation depends on the density in a complicated nonlinear manner. Therefore, well-known nonlinear phenomena can be expected in dense nonideal plasmas, such as ionization fronts, nonequilibrium phase separation, dissipative structures, etc.

Let us study the effect of nonideality, which means the influence of many-particle effects on the ionization kinetics in a dense hydrogen plasma. Our starting point is the reaction-diffusion equation (54) with the ionization and recombination coefficients (38) and (31) and the diffusion coefficient (57). It is convenient to use dimensionless variables for density, time, and length. We introduce a characteristic time $t_0=(\alpha^{\mathrm{id}}n)^{-1}$ and a characteristic length (diffusion length) $l_0=\sqrt{D^0_{\mathrm{AMB}}/t_0}$. Typical values, e.g., for $T=16\,000$ K and $n=10^{23}$ cm$^{-3}$ are $t_0\sim10^{-11}$ sec and $l_0\sim10^{-9}$ m. The dimensionless variables are now defined according to

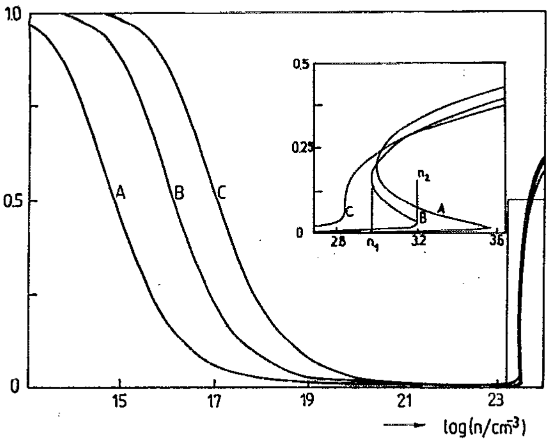

FIG. 7. Isotherms of the degree of ionization for (a) $T=10\,000$ K, (b) 12 000 K, (c) 14 000 K. The insert shows the density interval $[n_1,n_2]$ inside of which bistability occurs.

$$c=\frac{n_e}{n},\quad \frac{t}{t_0}\rightarrow t,\quad \frac{x}{l_0}\rightarrow x,\quad D=\frac{D_{\text{AMB}}}{D^0_{\text{AMB}}}.$$

Then we can transform the one-dimensional RDE into

$$\frac{\partial c}{\partial t}=\frac{d^2c}{dx^2}+W(c,n,T)=\frac{d^2c}{dx^2}+\frac{dU}{dc}\qquad(59)$$

with the hydrogen source function

$$W(c,n,T)=c\{(1-c)\exp[-(\Delta_e+\Delta_p-\Delta_H)/k_BT]$$
$$-\Lambda^3c^2\exp(-E_1/k_BT)\}$$

and the potential $U$ defined by $W=dU/dc$. The density dependence of the diffusion term gives only a minor effect and will be considered below.

Obviously, the behavior of the solutions of this equation is essentially determined by the zeros $c_m(n,T)$ of the source function. Especially, the $c_m$ determine the properties of the stationary solutions of the RDE. First we find the trivial zero $c_m=0$ corresponding to the atomic gas state which is always unstable. Further zeros have to be obtained from

$$\frac{c_m-1}{c_m^2}=\Lambda^3\exp[(-E_1+\Delta_H-\Delta_e-\Delta_p)/k_BT].\qquad(60)$$

This is just the Saha equation of the ionization equilibrium in a nonideal dense hydrogen plasma. The solutions of (60) are well investigated.[33,5,6] In Fig. 7, the isotherms $c_m(n,T)$ are shown which are the solutions of (60). A well-known property[33] of these isotherms is the following: For $T<T_{\text{crit}}$ and $n_I(T)<n<n_{II}(T)$, we obtain three zeros: $c_1<c_2<c_3$, where $c_1$ and $c_3$ correspond to stable stationary states while $c_2$ represents an unstable one. That means we observe a transition from monostable to bistable behavior in a density–temperature region which is shown in Fig. 8.

The bistable behavior has a number of interesting consequences. Let us first consider the stationary reaction-diffusion equation

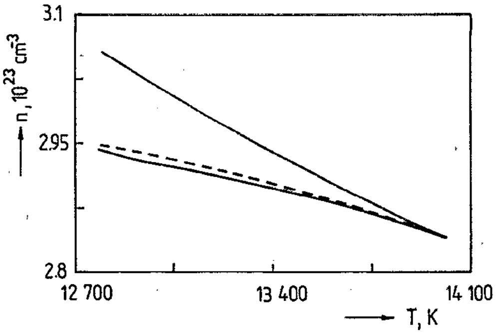

FIG. 8. Region of bistability in the density–temperature plane. The dashed line marks equal stability of the states $c_1$ and $c_3$ by the Maxwell construction. Above this line $c_3$ is more stable than $c_1$.

$$\frac{d^2c}{dx^2}=-W(c,n,T)=-\frac{dU(c,n,T)}{dc}.$$

The solution to this equation is known due to the obvious analogy with the Newton equation of motion for a particle of mass $m=1$ in the potential $U(c,n,T)$. We find for the density profile

$$x(c)=\int^c\frac{d\bar{c}}{\sqrt{2[E-U(\bar{c},n,T)]}}$$

with

$$E=\frac{1}{2}\left(\frac{\partial c}{\partial x}\right)^2+U(c,n,T).\qquad(61)$$

The integral of motion $E$ has to be determined from the boundary conditions, using the relation

$$L(E)=\int_{c^{(1)}}^{c^{(2)}}\frac{1}{\sqrt{2[E-U(c,n,T)]}}\,dc,\qquad(62)$$

where $L(E)=x_2-x_1$ is the length of the system. For example, we have, for Dirichlet boundary conditions $c(x_1)=c^{(1)}$ and $c(x_2)=c^{(2)}$, a unique relation between $L$, the boundary values $c^{(1)}$, $c^{(2)}$, and the constant $E$.

Let us now consider a plasma inside of the region of bistability under the following special boundary conditions:

$$c(x_1)=c_1,\quad c(x_2)=c_3,\qquad(63)$$

with $W(c_1)=W(c_3)=0$ and

$$\frac{\partial W(c_1)}{\partial c}<0,\quad \frac{\partial W(c_3)}{\partial c}<0,$$

with $c_1$ and $c_3$ being the stable zeros of $W$ and, therefore, local maxima of the potential $U(c_1)=\max$, $U(c_3)=\max$. Furthermore, the system is considered to be closed,

$$\left.\frac{\partial c(x)}{\partial x}\right|_{x=x_1}=\left.\frac{\partial c(x)}{\partial x}\right|_{x=x_2}=0.\qquad(64)$$

In this special case, (i) the boundary conditions (63) and (64) may be fullfilled only under the condition

$$E=U(c_1)=U(c_3),$$

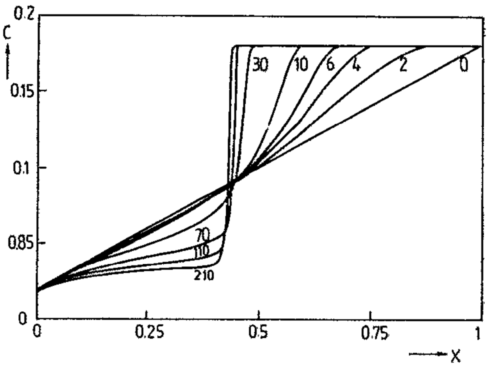

FIG. 9. Numerical solution of the RDE starting from a smooth profile and approaching a stationary kink, $D=1$, $T=13\,500$ K, $n\simeq n_{eq}=2.895\times10^{23}$ cm$^{-3}$. The number of time steps are shown, the time unit is $t_0\simeq6\times10^{-11}$ sec, the diffusion length $l_0\simeq7\times10^{-7}$ m.

i.e.,

$$\int_{c_1}^{c_2} W(c)dc=\int_{c_2}^{c_3} W(c)dc, \tag{65}$$

which corresponds to a Maxwell construction, $c_2$ being the unstable zero of $W$; (ii) condition (65) is fulfilled along a line $n_{eq}(T)$ marking equal stability of the stationary concentrations $c_1$ and $c_3$ (dashed line in Fig. 8);[34] (iii) the length $L$ of the system must be infinite [expand $U(c)$ around $c_E$ with $U(c_E)=E$]; (iv) one can even use a finite length $L=x_2-x_1$ if $L\gg l_0$. Here $l_0$ is very small in our case, indeed (see above).

Such a special solution is shown in Fig. 9, it is known as the "kink solution." Here, the kink describes a spatial phase separation between phases of different degrees of ionization $c_1$ and $c_3$. For stationary solutions with arbitrary boundary conditions, the constant $E$ and the boundary values $c(1)$ and $c(2)$ have to be determined self-consistently from (61) and (62).

Let us consider now the time-dependent solution of (59). If we leave the line $n_{eq}(T)$, changing density and temperature, the phase separation boundary is no longer at rest but starts moving with a velocity increasing drastically on approaching the edge of the bistability region (Fig. 8). Above this line, i.e., for $n>n_{eq}(T)$, the state $c_3$ is more stable than $c_1$, and the phase boundary is moving toward the phase of $c_1$ superseding it by the concentration $c_3$, and vice versa below the line. This can be seen in Fig. 10. This picture resembles an ionization front of the form

$$c(x,t)=c(x-vt)$$

describing the propagation of a density profile without deformation. Introducing this ansatz into (59), we come to a well-studied eigenvalue problem (in the mechanical analogy, the velocity term corresponds to a friction contribution)

$$c''+vc'=-\frac{\partial}{\partial c}U, \quad v=\text{const}. \tag{66}$$

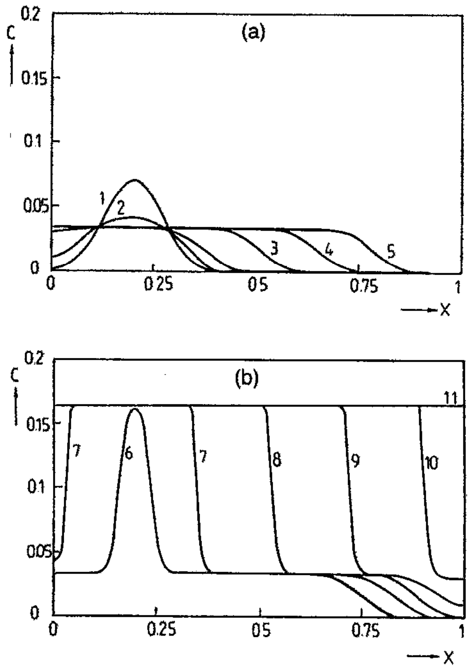

FIG. 10. Numerical solution of the RDE for $T=13\,500$ K and $n=2.9\times10^{23}$ cm$^{-3}>n_{eq}$ (spherical symmetry, vanishing particle fluxes at the boundaries). The initial profile is the (unstable) atomic gas with an undercritical fluctuation with respect to the stable state $c_3$. Part (a) shows droplet growth of the metastable state $c_1$, forming a spherical front. In part (b) an overcritical fluctuation is switched on generating a second much faster front. In the stationary state the plasma reaches a homogeneous profile $c(r)=c_3$. The time interval is always the same $\Delta=400$ steps, units same as in Fig. 9.

In general, Eq. (66) cannot be solved analytically, even for constant diffusion. Only for a few types of reaction functions exact results are known, e.g., for certain polynomials of integer or half-integer powers. For nonideal plasmas, a polynomial fit for the source function like the one used in Ref. 34 applies only within a narrow vicinity of the critical point.

We solved the time-dependent RDE (59) numerically for various initial distributions and boundary conditions. We present two of these calculations in Figs. 9 and 10 covering the most typical situations. Figure 9 shows a smooth initial profile with the concentration varying over a distance comparable with the total system length. No front solutions are possible in this case, and one observes a continuous approach of the asymptotic step profile. Fronts are observed only for a peaklike initial density distribution (with a width much less than the system length), as shown in Fig. 10(b). The time evolution consists of three stages. First, the automodal profile forms rather quickly, moving then a long time with a nearly constant velocity without deformation until it deforms into the stationary shape near the boundary.

An interesting property of the source function for hydrogen is that it has four zeros. This gives the possibility of three different types of running fronts choosing two of the three concentrations $c_0=0$, $c_1$ and $c_3$ as boundary values.[34,35] If one fixes the concentration to be $c_0$ (atomic gas) at one side of the system and to be $c_3$ at the other, the propagation of even two fronts becomes possible running one after another. This can be seen in Fig. 10(b) where the front superseding $c_0$ is followed by a second one which replaces $c_1$ by $c_3$. Choosing the parameters (density and temperature) appropriately, one can change the velocity and even the direction of the second front nearly arbitrarily.

Another phenomenon in bistable reaction-diffusion systems, however, in the two or three-dimensional case, is droplet growth. In one-dimensional systems, the replacement of one phase by another more stable one is proceeding spontaneously, whereas in higher dimensions it is impeded by surface effects. Indeed, diffusion acts to minimize the surface or more precisely the curvature of a density profile. It is dominating on small scales supressing small fluctuations. The well-known consequence is that there exists a critical droplet size (e.g., a critical radius for spherical droplets). Fluctuations of the more stable phase have to exceed this critical size in order to supersede the metastable phase. The critical droplet radius and the growth velocity can be estimated with the help of the formulas ($k=2$ for cylindrically and $k=3$ for spherically symmetrical nuclei, respectively)

$$R_{\mathrm{cr}}=-(k-1)\frac{\int_{c_1}^{c_3}(\partial c/\partial r)dc}{\int_{c_1}^{c_3}W(c,n,T)dc}, \tag{67}$$

$$\frac{dR}{dt}=(k-1)\left(\frac{1}{R_{\mathrm{cr}}}-\frac{1}{R(t)}\right). \tag{68}$$

The results hold for droplets with very thin transition region compared with the radius $\Delta \ll R$, i.e., for density profiles of the shape[36]

$$c(r,t)=\begin{cases} c_1, & r<R(t)-\Delta/2, \\ c_3, & r>R(t)+\Delta/2, \end{cases}$$

if $c_1$ is the stable and $c_3$ the metastable phase (in the opposite situation one has to substitute $c_1 \rightleftharpoons c_3$). This strong approximation fits very well for the nonideal plasma under consideration.

It is clear from (68) that small droplets ($r<R_{\mathrm{cr}}$) will vanish, but supercritical ones ($r>R_{\mathrm{cr}}$) will grow further. The solution of (68) gives the growth law

$$t=\frac{R_{\mathrm{cr}}^2}{k-1}\left(\ln\frac{R(t)-R_{\mathrm{cr}}}{R(0)-R_{\mathrm{cr}}}+\frac{R(t)-R(0)}{R_{\mathrm{cr}}}\right). \tag{69}$$

For small times there is a linear connection

$$R(t)\approx R_0+t\,\frac{k-1}{R_{\mathrm{cr}}}\,\frac{R(0)-R_{\mathrm{cr}}}{R(0)}. \tag{70}$$

After a transition time, the asymptotic growth of supercritical nuclei is again linear, however faster, since surface effects are of less importance:

$$R(t)\approx R(0)+t\,\frac{k-1}{R_{\mathrm{cr}}}. \tag{71}$$

The dynamics of subcritical droplets is, at the first stage, given by (70), too; after this, the shrinkage accelerates and cannot be described within this model. In Fig. 10, a numerical run is given showing droplet growth. The parameters are chosen above the line $n_{\mathrm{eq}}(T)$, i.e., the state $c_1$ is metastable, $c_3$ is stable. The initial profile [Fig. 10(a)] corresponds to atomic hydrogen with a single density fluctuation being undercritical with respect to $c_3$. Therefore, a spherical droplet of phase $c_1$ is growing first with a nearly constant velocity. In Fig. 10(b), we "switch on" a new but supercritical fluctuation, and a new spherical droplet (spherical front) starts growing running after the first one.

Now let us remember that, due to nonideality, the real diffusion coefficient $D_{\mathrm{AMB}}$ is not a constant but a nonlinear function of density with a minimum. Now even the stationary one-dimensional problem cannot be integrated,

$$Dc''+\frac{dD}{dc}(c')^2=-\frac{d}{dc}U, \tag{72}$$

since it is—speaking again in the mechanical picture—dissipative with the friction coefficient $dD/dc$.

As shown in Fig. 5, the diffusion coefficient can become negative indicating a mechanical instability and a phase transition. A peculiarity of hydrogen is, at least within our model, that bistability of the source function is always accompanied by negative values of $D_{\mathrm{AMB}}$. However, the diffusion terms on the lhs of (72) are smaller than the reaction terms (rhs) by several orders of magnitude (absolute values). The effect is the following: The evolution of the density profile in time proceeds on the first stage like one with $D=\mathrm{const}>0$ forming a kink (see above). Only when the step has become steep enough, the diffusion contribution is going to be of the same order as the reaction terms. The result is a rapid increase of fluctuations until the density has reached the values $c_1$ or $c_3$ being stabilized by the reactions.

## VII. CONCLUSIONS

Quantum statistical theory has shown the possibility of bistable ionization–recombination reactions as well as negative diffusion in a strongly coupled hydrogen plasma. These results have been obtained starting from kinetic equations which account for the formation and the decay of bound states as well as many-body effects. Generalized expressions could be derived for the coefficients of ionization and diffusion exhibiting an additional density dependence due to the influence of the surrounding plasma. The evolution of the number densities of the plasma species in space and time was then described by a reaction-diffusion equation that is valid for strongly coupled plasmas, too. It turns out that many-body effects are the reason for interesting nonlinear phenomena like front propagation, phase separation, and droplet growth. These phenomena are nonequilibrium counterparts of the equilibrium plasma phase transition. However, a strong theoretical description of the kinetics of this phase transition is still lacking since it cannot be found within the model of closed reaction-diffusion equations presented in this paper. Especially, we have to drop the assumption of homogeneous pressure. A further problem is to take into account the spatial and temporal evolution of temperature, what will be done in a forthcoming paper.

## ACKNOWLEDGMENTS

This work was carried out under the auspices of the Sonderforschungsbereich "Physikalische Grundlagen der Niedertemperaturplasmen" and was financed in part by the Deutsche Forschungsgemeinschaft.

## APPENDIX: THE CHEMICAL POTENTIALS FOR HYDROGEN

In this appendix, the interpolation formulas that were used for the calculation of the chemical potentials in a hydrogen plasma are given.

All formulas are written in Rydberg units:

$$\frac{e^2}{4\pi\varepsilon_0}=2,\quad m_e=\frac{1}{2},\quad \hbar=1,\quad \beta=\frac{\text{Ry}}{k_BT}.$$

The chemical potentials were split into ideal and interaction contributions $\mu_a = \mu_a^{\text{id}} + \mu_a^{\text{int}}$. The ideal parts are determined according to the standard expressions.

For the correlation parts of electrons and protons, we have made use of Padé formulas of Ebeling and Richert (cf., e.g., Ref. 20) given in an explicit form in.[37]

For the correlation contribution of the electron gas, the following Padé formula is a good approximation:

$$\mu_e^{\text{int}}=\frac{\mu_{eD}-\frac{1}{2}(\pi\beta)^{-1/2}\bar{n}_e+8\mu_{GB}\bar{n}_e^2}{1+8\ln[1+(1/16\sqrt{2})(\pi\beta)^{1/4}(\bar{n}_e)^{1/2}]+8\bar{n}_e^2} \tag{A1}$$

with the abbreviations:

$$\bar{n}_e=n_e(4\pi\beta)^{3/2},\quad r_s=\left(\frac{3}{4\pi n_e}\right)^{1/3},$$

$$\mu_{eD}=-(\pi\beta)^{-1/4}\bar{n}_e^{1/2},$$

$$\mu_{GB}=-\frac{1.2217}{r_s}-0.088\,83\ln\left(1+\frac{6.2208}{r_s^{0.7}}\right).$$

The result for the proton gas is

$$\frac{\mu_p^{\text{int}}}{k_BT}=\frac{(\mu_{pD}/k_BT)[1-2a\tilde{n}_p^{2/3}(\mu_{MC}/k_BT)]}{1-2a\tilde{n}_p^{1/2}[\tilde{n}_p^{1/2}/(\mu_{pD}/k_BT)+\tilde{n}_p^{1/6}(\mu_{pD}/k_BT)]} \tag{A2}$$

with

$$\tilde{n}_p=8\beta^3n_p,\quad \Gamma=(\tfrac{4}{3}\pi\tilde{n}_p)^{1/3},$$

and

$$a=\sqrt{\frac{\pi^3}{\beta}}\left\{\frac{1}{2}\left[1+\frac{1}{\sqrt{4\pi\beta}}\exp\left(\frac{3\sqrt{\pi}}{\ln(4\beta)-6\sqrt{4\beta}}\right)\right]\right.$$
$$\left.-0.299\,31\right\},$$

$$\mu_{pD}=-\tfrac{3}{2}\cdot 2.1605(\tilde{n}_p)^{1/2},$$

$$\frac{\mu_{MC}}{k_BT}=-1.1928\Gamma+3.5382\Gamma^{1/4}-0.5012\ln(\Gamma)$$
$$-2.9761-\frac{r_s\tilde{n}_p^{1/3}}{1+(r_s)^2}[0.0933$$
$$+0.8206(\tilde{n}_p)^{-1/4}-0.2287(\tilde{n}_p)^{-1/3}].$$

For the interaction contribution of the atomic chemical potential, the model of effective hard spheres with temperature-dependent diameters $d_H(T)$ according to Carnahan and Starling[38] was used:

$$\frac{\mu_H^{\text{int}}}{k_BT}=y\frac{8-9y+3y^2}{(1-y)^3} \tag{A3}$$

with the packing fraction parameter $y=(\pi/6)n_H[d_H(T)]^3$. The diameters $d_H$ were determined following Barker–Henderson theory.[39]

[1] *Strongly Coupled Plasmas*, edited by G. Kalman and P. Carini (Plenum, New York, 1978).

[2] *Strongly Coupled Plasma Physics*, edited by F. I. Rogers and H. E. DeWitt (Plenum, New York, 1987).

[3] *Strongly Coupled Plasma Physics*, edited by S. Ichimaru (Elsevier Science B.V./Yamada Science Foundation, Amsterdam, 1990).

[4] V. E. Fortov and I. T. Yakubov, *Physics of Nonideal Plasmas* (Academy of Science, Chernogolovka, 1984).

[5] W. Ebeling, W.-D. Kraeft, and D. Kremp, *Theory of Bound States and Ionization Equilibrium in Plasmas and Solids* (Akademie-Verlag, Berlin, 1976).

[6] W.-D. Kraeft, D. Kremp, W. Ebeling, and G. Röpke, *Quantum Statistics of Charged Particle Systems* (Plenum, London, 1986).

[7] W. Ebeling, *Strukturbildung bei irreversiblen Prozessen* (Teubner, Leipzig, 1976).

[8] G. Nicolis and I. Prigogine, *Self-Organization in Nonequilibrium Systems* (Wiley, New York, 1977).

[9] P. C. Fife, *Mathematical Aspects of Reacting and Diffusing Systems*, Lecture Notes in Biomathematics (Springer-Verlag, New York, 1979), Vol. 28.

[10] S. V. Peletminski, Teor. Mat. Fiz. **30**, 123 (1971).

[11] J. T. Lowry and R. F. Snider, J. Chem. Phys. **61**, 2320, 2330 (1974).

[12] Yu. L. Klimontovich and D. Kremp, Physica A **109**, 517 (1981).

[13] Yu. L. Klimontovich, D. Kremp, and W.-D. Kraeft, Adv. Chem. Phys. **58**, 175 (1987).

[14] J. A. McLennan, J. Stat. Phys. **57**, 887 (1989).

[15] M. Schlanges, Habil thesis, Rostock University, 1985.

[16] T. Bornath, Ph.D. thesis, Rostock University, 1987.

[17] D. Kremp, M. Schlanges, and T. Bornath, in *Proceedings of the ZIE-Scool on Kinetic Equations and Nonlinear Optics in Semiconductors*, edited by H. Stolz (Zentralinstitut Elektronenphysik, Berlin, 1986), p. 33.

[18] M. Schlanges and T. Bornath, "Ionization and recombination coefficient in a dense nonideal hydrogen plasma. Effects of screening and degeneracy," Physica A (in press).

[19] R. Zimmermann, *Many-Particle Theory of Highly Excited Semiconductors* (Teubner, Leipzig, 1987).

[20] W. Ebeling and W. Richert, Phys. Status Solidi B **128**, 467 (1985).

[21] G. E. Norman and A. N. Starostin, High Temp. Phys. **6**, 410 (1968) (in Russian).

[22] G. E. Norman and A. N. Starostin, High Temp. Phys. **8**, 413 (1970) (in Russian).

[23] K. Kilimann, W.-D. Kraeft, and D. Kremp, Phys. Lett. A **61**, 393 (1977).

[24] R. Zimmermann, K. Kilimann, W.-D. Kraeft, D. Kremp, and G. Röpke, Phys. Status Solidi B **90**, 175 (1978).

[25] K. Kilimann, D. Kremp, and G. Röpke, Teor. Mat. Fiz. **55**, 448 (1983).

[26] M. Schlanges, T. Bornath, and D. Kremp, Phys. Rev. A **38**, 2174 (1988).

[27] T. Bornath, M. Schlanges, and D. Kremp, Contrib. Plasma Phys. **28**, 57 (1988).

[28] Yu. L. Klimontovich, M. Schlanges, and T. Bornath, Contrib. Plasma Phys. **30**, 349 (1990).

[29] D. Kremp, M. Schlanges, and T. Bornath, in *The Dynamics of Systems with Chemical Reactions*, edited by J. Popielawski (World-Scientific, Singapore, 1989), p. 3.

[30] M. Schlanges, T. Bornath, M. Bonitz, and D. Kremp, in *Far-From-Equilibrium Dynamics of Chemical Systems*, edited by J. Popielawski (World-Scientific, Singapore, 1991), p. 192.

[31] The zeroth order gives no contribution to the diffusion coefficients.

[32] M. Bonitz, Ph.D. thesis, Rostock University, 1990.

[33] W.-D. Kraeft, K. Kilimann, and D. Kremp, Phys. Status Solidi B **72**, 461 (1975).

[34] W. Ebeling, A. Förster, D. Kremp, and M. Schlanges, Physica A **159**, 285 (1989).

[35] M. Bonitz, C. Kremp, and D. Kremp, Wiss. Z. Universität Rostock **6**, 90 (1989).

[36] L. Schimansky-Geier and W. Ebeling, Ann. Phys. (Leipzig) **40**, 10 (1983).

[37] P. Haronska, D. Kremp, and M. Schlanges, Wiss. Z. Universität Rostock **36**, 98 (1987).

[38] N. F. Carnahan and K. E. Starling, J. Chem. Phys. **51**, 635 (1969).

[39] J. A. Barker and D. Henderson, J. Chem. Phys. **47**, 4714 (1967).